Drug Design, Development and Therapy

Dovepress
open access to scientific and medical research

Open Access Full Text Article

ORIGINAL RESEARCH

Metabolomics Provides Insights into Renoprotective Effects of Semaglutide in Obese Mice

Xing Chen[1], Shuchun Chen[2,3], Qingjuan Ren[3], Shu Niu[3], Xiaoyu Pan[3], Lin Yue[3], Zelin Li[3], Ruiyi Zhu[3], Zhuoya Jia[3], Xiaoyi Chen[3], Ruoxi Zhen[3], Jiangli Ban[3]

[1]Department of Nephrology, Hebei General Hospital, Shijiazhuang, 050051, People's Republic of China; [2]Department of Endocrinology, Hebei General Hospital, Shijiazhuang, 050051, People's Republic of China; [3]Department of Internal Medicine, Hebei Medical University, Shijiazhuang, 050017, People's Republic of China

Correspondence: Shuchun Chen, Department of Endocrinology, Hebei General Hospital, 348 Heping West Road, Shijiazhuang, Hebei, 050051, People's Republic of China, Tel/Fax +86 311 85988406, Email chenshuchunwork88@163.com

Purpose: Semaglutide, a new long-acting glucagon-like peptide-1 analogue, has shown benefits for renal diseases, but its direct role on kidney metabolism under obesity remains unclear. The study aims to elucidate the protective effect and metabolic modulation mechanism of semaglutide on obesity-related kidney injury.

Methods: Male C57BL/6J mice were divided into control and obesity groups. Mice in the obesity group had a high-fat diet and were treated with or without semaglutide (30nmol/kg/day). The study assayed blood biochemistry and then evaluated renal pathological injury through Periodic Acid-Schiff staining and electron microscopy. Metabolomics was utilized to analyze obesity-related metabolites in kidney samples.

Results: Semaglutide significantly improved glucose homeostasis, insulin resistance, and kidney injury in obese mice. We successfully identified 377 altered metabolites ($P<0.05$). It was suggested that semaglutide directly improved oxidative stress and inflammation-related metabolites such as nicotinamide adenine dinucleotide (NAD^+) and adenosine in the kidney of obese mice, which have not been documented in obesity-related kidney injury. Relevant enriched pathways were included phospholipids and lysophospholipids metabolism, purine metabolism, NAD^+ metabolism, and insulin resistance-related metabolism. They could serve as potential targets for intervention of obesity-related kidney injury.

Conclusion: Our study revealed the metabolomics-based renoprotective mechanism of semaglutide in obese mice for the first time. The innovation lied in the identified metabolites such as NAD^+ and adenosine targeted by semaglutide, which have not been documented in obesity-related kidney injury. Semaglutide may be a promising therapy for obesity-related kidney diseases.

Keywords: semaglutide, glucagon-like peptide-1, metabolomics, obesity, kidney

Introduction

Epidemiologic studies have reported that obesity, a public health issue worldwide, contributes to cardiovascular diseases, diabetes mellitus, and many other chronic diseases with high mortality.[1–3] High body mass index is an independent risk factor for the onset and progression of chronic kidney disease (CKD),[4] and may directly lead to obesity-related glomerulopathy (ORG).[5,6] With the increased number of patients with obesity, the prevalence of ORG is also surging. ORG is characterized by mesangial expansion and glomerular hypertrophy with or without secondary focal segmental glomerulosclerosis under light microscopy. Electron microscopy can observe increased foot-process width with decreased podocyte density.[1,3,6] Podocyte injury has been considered a hallmark of ORG and plays a pivotal role in the progression of ORG,[5,6] whereas the detailed mechanisms of ORG are complex and not well understood. Hence, the exploration of intervention targets for early prevention and treatment on ORG is of critical importance.

Received: 23 July 2022
Accepted: 29 October 2022
Published: 9 November 2022

DPP-4 inhibitors are correlated with lower risks of decreased renal function in patients with type 2 diabetes and have protective effects on renal complications.[7] Glucagon-like peptide-1 (GLP-1), which is an intestinal peptide hormone that is secreted by L, can influence insulin synthesis, appetite, and weight loss. GLP-1 can inhibit autophagy induced by hyperglycemia and decrease free fatty acid concentration.[8,9] In patients with diabetic peripheral neuropathy and atherosclerosis, GLP-1 concentrations were reduced significantly.[10–12] Liraglutide is an acylated GLP-1 analogue and is approved for once-daily treatment of diabetes as well as obesity.[9–14] Semaglutide is a newer GLP-1 analogue that is further optimized for high-affinity albumin binding, and it is allowed for once-weekly administration due to a greatly prolonged half-life of 165 hours in humans.[15–17] Current studies about semaglutide focus on cardiovascular disease and non-alcoholic fatty liver disease.[16,18–20] However, the renoprotective effect of semaglutide and its involved mechanisms remain unclear.

Metabolomics is a systemic biological approach that provides global metabolic information and instantaneous changes within the organism. This approach has been widely used in diagnosis, prediction, and treatment efficacy evaluation in many diseases.[21,22] Several analytical methods, including nuclear magnetic resonance spectroscopy (NMR), gas chromatography coupled mass spectrometry (GC-MS), and liquid chromatography coupled mass spectrometry (LC-MS), are used in metabolomic studies.[23] Recent metabolomic studies reported that several combined plasma and urine metabolites could predict development of macroalbuminuria in diabetes patients.[21–24] Up to now, no study has investigated the detailed action at the metabolic level of semaglutide acting on ORG. Thus, metabolomics may potentially bring an innovative view on the efficacy concerning the renoprotective effects of semaglutide.

This study aims to evaluate the renal protective effect of semaglutide in obese mice induced by high-fat diet (HFD). We applied untargeted metabolomics, integrated with conventional clinical chemistry, histological and biological methods to reveal significant metabolic biomarkers and pathways involved.

Research Design and Methods

Ethical Statement

All animal care and experiments were conducted under the institutional guidelines. All animal work was approved by the Animal Care and Treatment Committee of Hebei General Hospital (Shijiazhuang, China).

Chemicals and Reagents

Semaglutide was purchased from Novo Nordisk A/S. Serum creatinine (Scr) kits, uric acid (Ua) kits, triglyceride (TG) kits, total cholesterol (TC) kits, high-density lipoprotein (HDL) kits, low-density lipoprotein (LDL) kits, superoxide dismutase (SOD) kits, and malondialdehyde (MDA) kits were obtained from Nanjing Jiancheng Bioengineering Institute (Nanjing, China). Mouse insulin elisa kits and mouse microalbumin (MAU) kits were from Wuhan Ilerite Biotechnology Co., LTD (Wuhan, China). Mouse interleukin-1β (IL-1β) kits, mouse interleukin-6 (IL-6) kits, and mouse tumor necrosis factor-α (TNF-α) kits were purchased from Hangzhou Lianke Biotechnology Co., LTD (Hangzhou, China).

Animals and Experimental Design

Six-week-old male C57BL/6J mice were obtained from Hebei Invivo Biological Technology Co., LTD (Shijiazhuang, China). The mice were reared in a conventional environment (temperature 22±1°C, relative air humidity 55±15%, and 12 hours/12 hours light/dark cycle from 7 AM to 7 PM) with free access to water. After acclimatization for 1 week, 10 mice were fed with normal-fat diet (NFD) (D1035, 10% of total calories from fat, Research Diets, Beijing Huafukang Biotechnology Co., LTD, China) and 18 mice were fed with HFD (H10060, 60% of total calories from fat, Research Diets, Beijing Huafukang Biotechnology Co., LTD, China) for 13 weeks. Obese mice were defined as those with a body weight >20% higher compared with the baseline weight of the control group.[13,18,25] All HFD mice were confirmed to be successful modeling in our study. After modeling, we randomly selected two mice from each group for glomerular pathology. The rest of mice were randomly divided into three groups as follows: NFD group (n=8), HFD group (n=8), fed HFD and administered with semaglutide group (HFDS) (n=8). HFDS group mice were assigned to subcutaneous administration of semaglutide (30nmol/Kg/d) once daily for 13 weeks. Body weights of mice were recorded on a weekly basis. We applied glucose tolerance tests after an additional 13 weeks of semaglutide intervention. Urine was obtained for

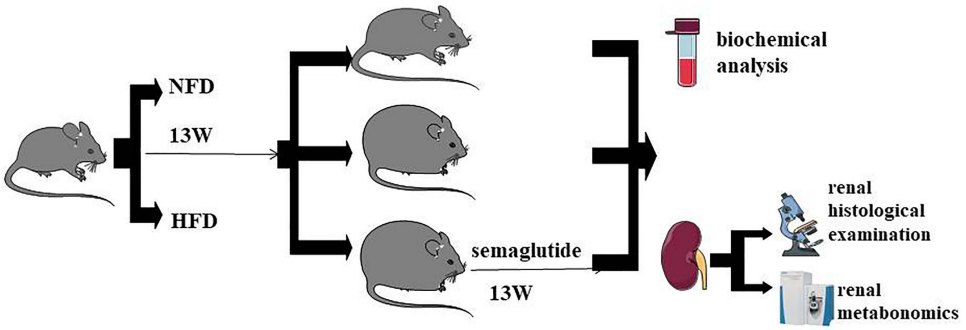

Figure 1 Flow chart of experimental design.

measurement of the urinary albumin/creatinine ratio (UACR). At the end of treatment, all mice were anesthetized with chloral hydrate (300mg/Kg), and the kidneys were rapidly removed. Measurement of Lee's Index and the body mass were performed. The body length (the distance from the tip of the nose to the anus) was accurately measured for the calculation of Lee's index according to the calculation formula: Lee's index=(body weight (g)×1000)$^{1/3}$/body length (cm).[25] Perirenal and periepididymal fat were isolated from the mice, and the abdominal fat index was calculated, where fat index=(perirenal fat+periepididymal fat)/body weight.[13] Portions of kidneys were obtained for metabolomics and pathological analysis. The specific flow chart was shown in Figure 1.

Intraperitoneal Glucose Tolerance Test

Intraperitoneal glucose tolerance tests (IPGTTs) were performed after 6 hours of fasting. The mice were given glucose (2 mg/g) intraperitoneally. We measured blood glucose levels from the tail vein at 0, 15, 30, 60, 90, and 120 minutes after glucose injection, and analyzed the area during IPGTT under the curve (AUC) from 0 min to 120 min (GraphPad Prism v.9.2; GraphPad Software, La Jolla, CA, USA). Homeostasis model assessment (HOMA) of insulin resistance and Quantitative Insulin Sensitivity index (QUICKI) were calculated as follows: HOMA=(fasting plasma glucose (mg/dL)×fasting plasma insulin (ng/mL))/405; QUICKI=1/ (log (INS0)+log (G0)), where INS0 is fasting insulin (μU/mL) and G0 is fasting blood glucose (mg/dL).[9,14,18,27]

Biochemical Analysis

At the end of the experiment, blood was collected immediately after removing the eyeballs. Levels of Scr, UA, TC, TG, HDL, LDL, urinary creatinine (Ucr), and MAU were measured using commercially available kits according to the manufacturer's instructions. UACR was further assessed by MAU and Ucr. The creatinine clearance (Ccr) was calculated as follows: Ccr=(Ucr×urine volume per minute)/Scr×100% (mL/min).[8]

Renal Histological Examination

Preparation of Kidney Sections for Light Microscopy

We obtained 3mm-thick kidney tissue and fixed it in a 4% paraformaldehyde phosphate buffer for 48 hours at room temperature. Fixation was followed by dehydration using ethanol in stages from 70% to 100%, clearing in xylene, and embedding in paraffin. The embedded renal tissues were cut into 5μm-thick sections. Renal sections were stained with hematoxylin and eosin (HE) and periodic acid-Schiff (PAS). The glomerular diameter and tubular injury index were calculated as previously reported. A total of 20 images of glomerular maximal profiles with vascular pole and/or urinary pole were randomly selected using a confocal microscope.[8,28] The longest diameter from urinary pole to vascular pole was recorded using the Image-Pro Plus Analysis software (Media Cybemetics, Image-Pro Plus 6.0, USA). The glomeruli were selected randomly by an experienced clinicopathologist.

In addition, images of 20 random visual fields containing only tubules and interstitium were captured (×200 magnification). We assessed the relative area of tubules displaying vacuolar degeneration or necrosis in each visual field using

a semi-quantitative method and calculated the mean value. A semi-quantitative method was described as the areas involved accounted for <25, 26–50, 51–75, and >75% of the visual field, which were given injury scores of 1, 2, 3, and 4, respectively.[6]

Oil Red O Staining

Kidney tissue was fixed in 4% paraformaldehyde, embedded, made to 5μm frozen sections, and then incubated with Oil Red O solution (KeyGen Biotech Co. Ltd., Nanjing, China) at 37°C for 20 min. After washing three times with PBS, the nuclei were counterstained with hematoxylin. The stained sections were assessed for the percentage of lipid droplet positive area.[5,6]

Transmission Electron Microscopy (TEM)

Kidney tissue samples were cut into $1mm^3$ cubes and fixed in a 2.5% glutaraldehyde solution in 0.1 M phosphate buffer. The blocks were washed three times in PBS, followed by 1% osmium acid fixation for 2 hours. Following dehydration with an ethanol series, the blocks were infiltrated by a 1:1 solution of anhydrous acetone and an embedding agent. Ultrathin sections (100nm) were obtained on copper grids and stained with tannic acid and lead solution.[5,6]

Renal Metabolomics Analysis

Preparation for Untargeted Metabolomics

A 30mg accurately weighed kidney sample was transferred to a 1.5mL Eppendorf tube. The samples were stored at −20°C for 2 minutes and grinded at 60 HZ for 2 minutes. The whole samples were extracted by ultrasonic in ice water bath for 10 minutes. The extract was centrifuged at 4°C (13,000 rpm) for 10 minutes. Samples were redissolved with 300μL methanol-water (V:V=1:4) (scroll 30s, ultrasonic 3min). The samples were centrifuged at 13,000 rpm for 10 minutes at 4°C. Supernatants were filtered (0.22μm) and stored at −80°C for LC-MS analysis. We prepared quality control (QC) samples to be a pooled sample by mixing aliquot of the all samples.[25,29]

LC-MS Conditions for Kidney Metabolomics

Kidney samples were analyzed using a Waters ACQUITY UHPLC system coupled with a QE High Definition Mass Spectrometer (Waters, USA). Chromatographic separation was archived on an ACQUITY UHPLC HSS T3 column (100mm×2.1 mm, 1.8um, Waters) with column temperature kept at 40°C and injection volume of 5uL. Mobile phases A and B were 0.1% formic acid (v/v) in water and acetonitrile, respectively. The flow rate was 0.35mL/min. The LC gradient was from 5% to 100% B in 12 minutes, kept at 100% B for 2 minutes then went back to the initial condition. All samples were maintained at 4°C during analysis, and a mass spectrometer with an ESI source was used for both positive and negative ions.[25,29]

Data Processing and Pattern Recognition Analysis

We applied Application Manager (Waters) to align data. A data matrix containing the peak intensity, mass, and retention time was generated. To recognize potential patterns, we utilized Principle Component Analysis (PCA) and Orthogonal Partial Least-Squares-Discriminant Analysis (OPLS-DA). The S-plots and Variable Importance of Projection (VIP)-plots based on OPLS-DA analysis were conducted to extract potential biomarkers. Parameters of R2Y and Q2 were used to evaluate the model. To screen the biomarkers, we performed Student's *t*-test between groups by SPSS (version 21.0) software. Then the potential biomarkers were identified by comparing precise mass-to-charger ratio (M/z), secondary fragments, and isotopic distribution with the standards from Human Metabolome Database (HMDB) database, Lipidmaps (v2.3), METLIN database and databases containing more than 4000 metabolite information self-built by Shanghai Lu-Ming Biotech Co., Ltd. The related metabolic pathways were further confirmed in KEGG database (http://www.genome.jp/kegg/pathway.html).

Correlation Analysis Between Clinicopathological Parameters and Identified Metabolites

Pearson statistical analysis was applied to assess the association between clinicopathological indicators such as UACR, Scr, glomerular diameter and identified metabolites.

Statistical Analysis

First, we performed the Shapiro–Wilk test and QQ plots for assessing normality. Parametric tests were used if the data had a normal distribution, and non-parametric tests were used if the data failed the normality test. Data were expressed as means±SD. For the comparison between two groups, Student's *t*-tests were used considering the normally distributed data. Among multiple groups, comparisons were performed by one-way analysis of variance (ANOVA) or non-parametric tests (Kruskal Wallis tests). Bonferroni test was used for post hoc comparisons. Values of $P<0.05$ were considered statistically significant. The statistical analysis of the metabolomics data for each sample was performed using the program mentioned above.

Results

Modeling Evaluation

After 13 weeks of HFD, body weight, Lee's index, and glomerular diameter of mice were analyzed to evaluate modeling. As shown in Figure 2, the body weight of mice in HFD began to increase significantly in the second week, and the difference was statistically significant. At the end of modeling, the body weight of mice in HFD group was significantly higher than that of the control group (43.35±3.23 vs 28.01±1.80, $P<0.001$). Increased glomerular volume, the proliferation of mesangial matrix, and necrosis of renal tubular epithelial cells were observed in HFD group under light microscopy. PAS staining showed that the glomerular diameter of HFD group was larger than that of NFD group (68.57±4.84μm vs 57.30±3.03μm, $P=0.001$) (Figure 3A–B). The Lee's index of mice in HFD group was higher than that of control group (3.40±0.75 vs 3.14±0.56, $P<0.001$) (Figure 3C). The obese model was successful.

Effect of Semaglutide on Body Weight and Body Composition

During semaglutide intervention, the body weight of HFDS group continued to decrease significantly, where it increased gradually in HFD group (NFD group: 27.98±1.23g, HFD group: 44.17±3.92g, HFDS group: 29.23±1.02g, $P<0.001$) (Figure 4). Multiple post-mortem comparisons showed that the differences between each group were all statistically significant. Figures 5 and 6showed that Lee's index, abdominal fat index, and the right kidney of mice increased after HFD, while decreased after semaglutide administration. The difference was statistically significant.

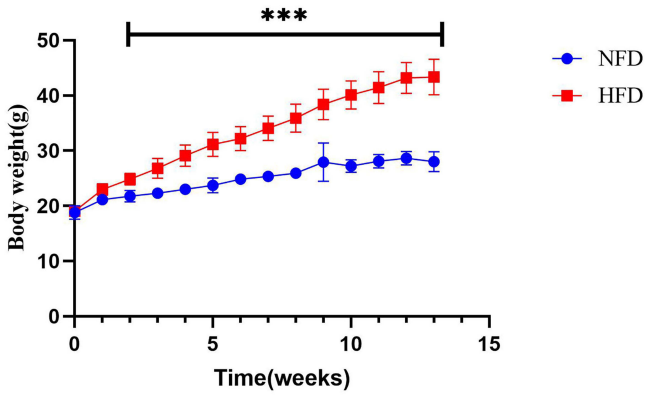

Figure 2 Body weight of NFD and HFD mice. ***P<0.001, compared with NFD group.

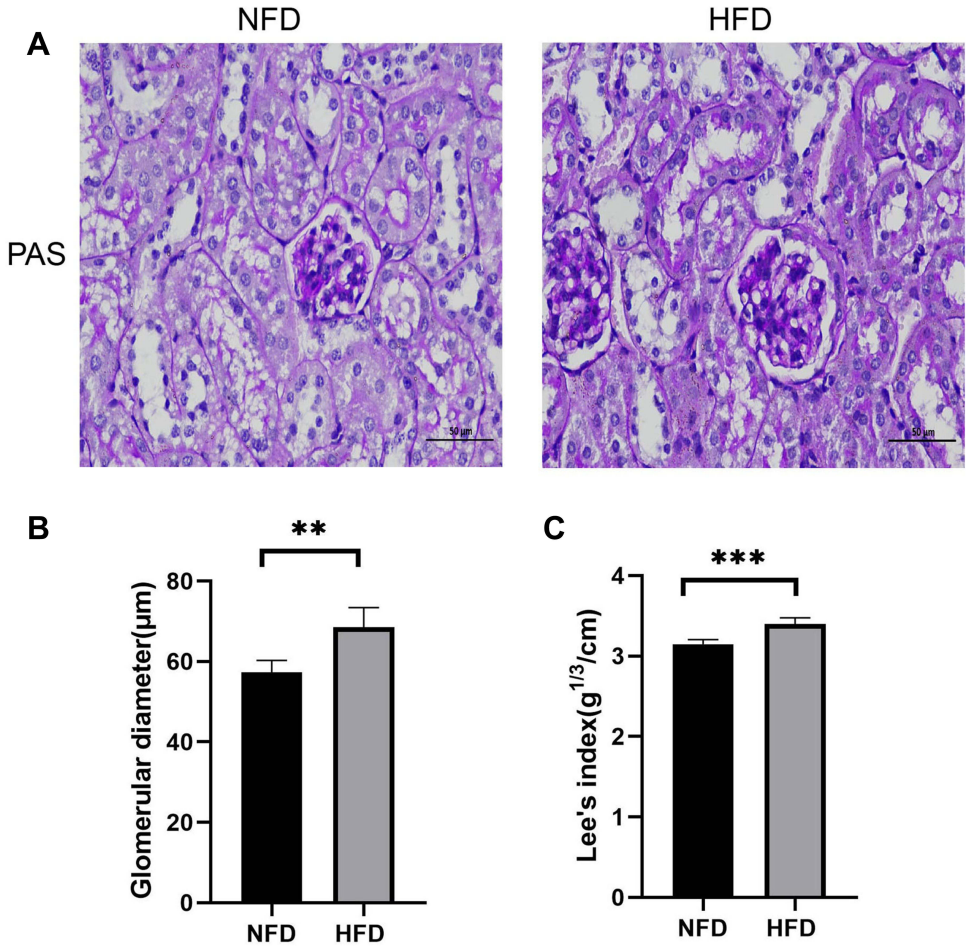

Figure 3 Lee's index and glomerular diameter of mice in HFD and NFD group. (**A**) Periodic acid-Schiff (PAS)-stained (×400 magnification). (**B**) Glomerular diameter of mice. (**C**) Lee's index of mice. **P<0.01, ***P<0.001, compared with NFD group.

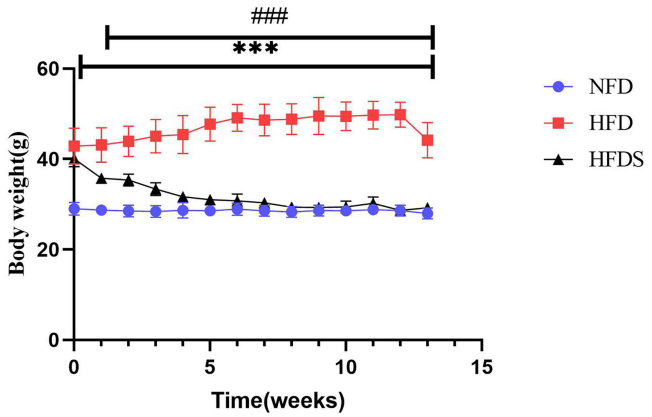

Figure 4 Effect of semaglutide on body weight. Means data from each group (n=8/group) are displayed ***P<0.001, compared with NFD group, ###P<0.001, compared with HFD group.

Effect of Semaglutide on Biochemical Parameters and Insulin Resistance

To evaluate the effect of semaglutide on ORG, the study compared the parameters of different groups (Table 1). The results showed that levels of Ua, G0, TC, LDL, HDL, and UACR in HFD group were much higher than those in NFD

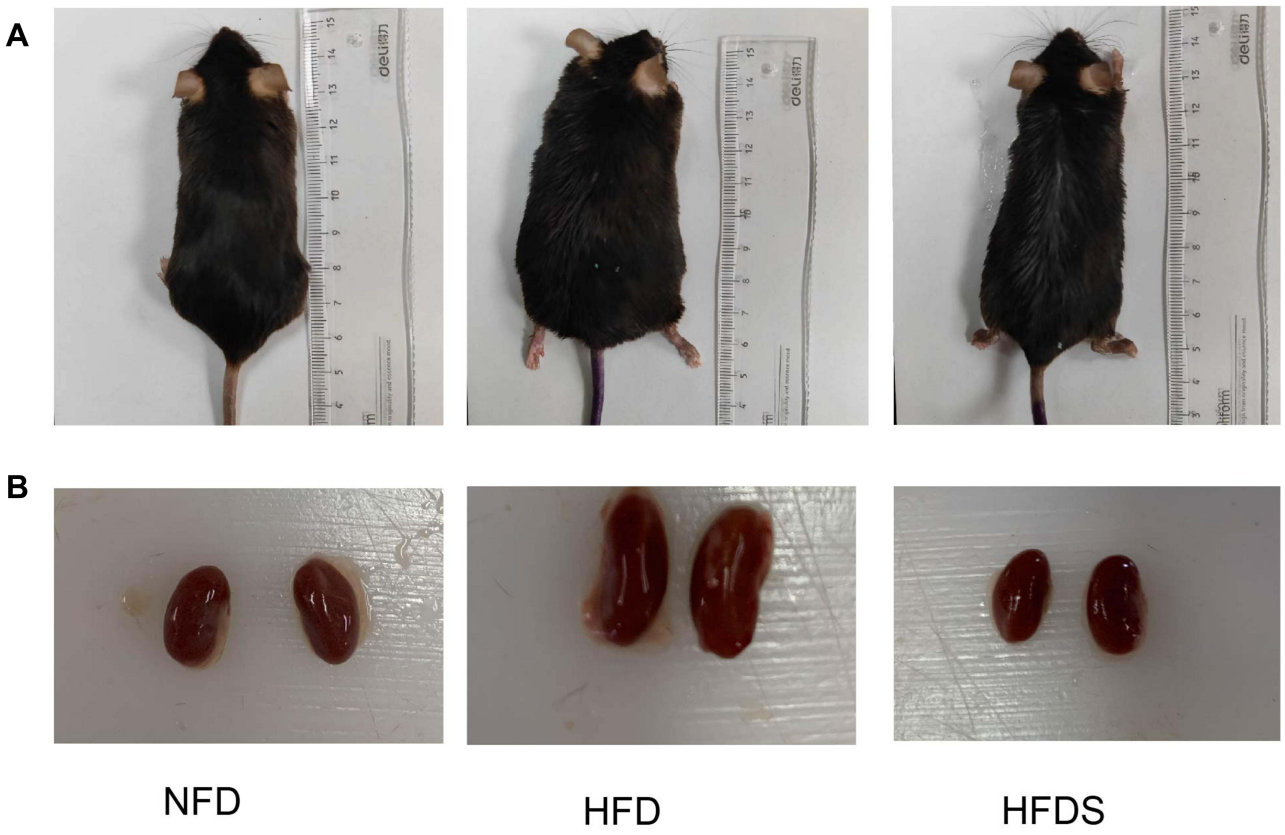

Figure 5 Effect of semaglutide on body weight and kidney of mice. (**A**) Gross appearance of mice in each group. (**B**) Kidney gross appearance in each group.

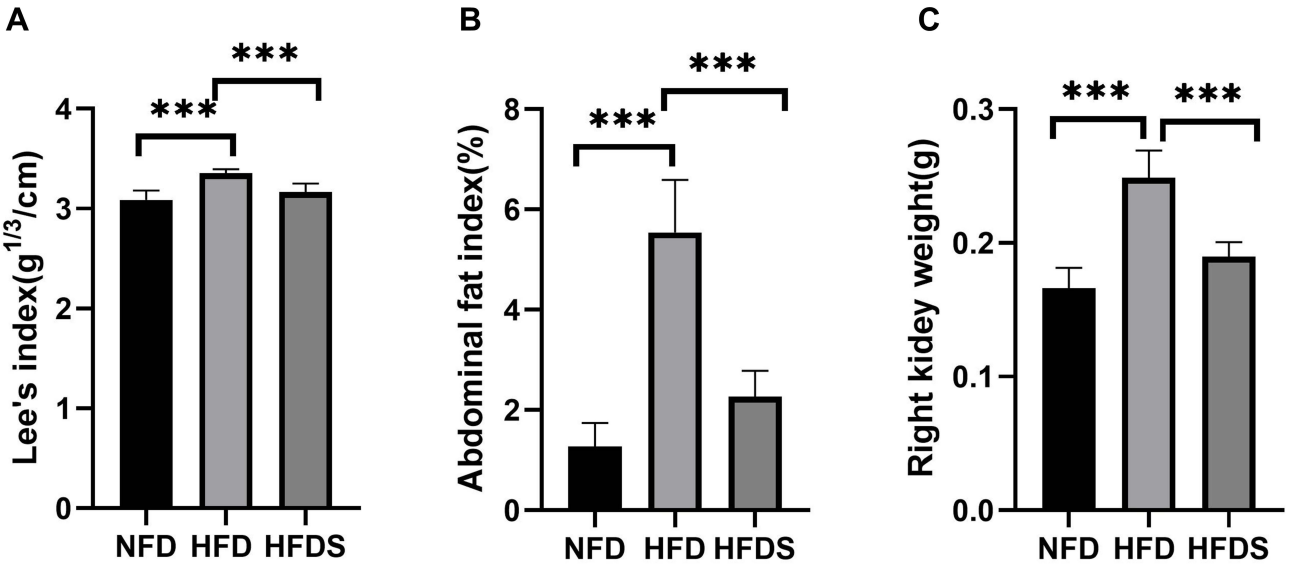

Figure 6 Effect of semaglutide on Lee's index, abdominal fat index and the right kidney weight. Means data from each group (n=8/group) are displayed ***P<0.001, compared with NFD or HFD group. (**A**) Lee's index in each group. (**B**) Abdominal fat index in each group. (**C**) Right kidney weight of mice in each group.

group, indicating the disordered metabolism in HFD mice. Semaglutide significantly decreased levels of these parameters. There was no statistical difference in Scr levels among groups.

This study showed that HFD mice had higher fasting blood glucose and fasting insulin than control mice. Although fasting blood glucose was higher in HFD group than NFD mice, it did not meet the criteria for diagnosis of diabetes. Semaglutide significantly reduced fasting insulin, but not fasting blood glucose. The AUC in HFD group was higher than NFD group, and semaglutide further reduced the area under AUC curve (NFD: 1619±78.59, HFD: 2667±119.8, HFDS:

Table 1 Effects of Semaglutide on Biochemical Parameters

Parameters	Scr (μmol/)	Ccr (mL/min)	Ua (μmol/)	TG (mmol/L)	TC (mmol/L)	LDL (mmol/L)	HDL (mmol/L)	UACR (mg/mmol)	INS0 (pg/mL)	G0 (mmol/L)
NFD	60.68 ±9.91	(2.01 ±0.62)%	138.19 ±23.97	0.64±0.10	3.15±0.39	2.19±0.47	2.86±0.61	0.18±0.06	300.05 ±44.02	4.36±0.59
HFD	62.72 ±11.46	(3.09 ±0.11)%*	254.63 ±42.34***	0.93 ±0.13***	8.36 ±1.23***	6.79 ±1.37***	6.94 ±1.18***	0.83±0.15***	411.69 ±143.500	7.86±1.65***
HFDS	61.37 ±9.66	(2.23 ±0.40)%	172.83 ±19.04###	0.72 ±0.16##	5.84 ±0.45####	4.78 ±0.45####	4.56 ±0.86####	0.38±0.13####	174.86 ±59.92####	6.74±1.52

Notes: *p<0.05, ***p<0.001, compared with NFD; ##p<0.01, ####p<0.001, compared with HFD.
Abbreviations: Scr, serum creatinine; Ua, uric acid; TG, triglyceride; TC, total cholesterol; HDL, high-density lipoprotein; LDL, low-density lipoprotein; Ccr, creatinine clearance; UACR, urinary albumin/creatinine ratio; INS0, fasting plasma insulin; G0, fasting blood glucose.

1626±130.9) (Figure 7). The HOMA index indicated insulin resistance and the QUICKI index indicated insulin sensitivity all revealed that the insulin signaling pathway was impaired. Semaglutide attenuated the insulin resistance induced by HFD as shown in Figure 7.

Effect of Semaglutide on Renal Histopathology

The increased glomerular volume, mesangial expansion, and vacuolated renal tubular epithelial cells were observed in HFD group under light microscope. Similarly, focal infiltration of lymphocytes was observed, but no obvious renal interstitium fibrosis in Masson stain in HFD group. It was showed expanded mesangial regions and increscent glomerular volume in HFD mice compared with NFD group. Semaglutide significantly mitigated the glomerular and tubular injury (Figure 8). The significant accumulation of oil red O-stainable lipid was discovered in HFD mice. Semaglutide contributed to the reduction of lipid droplets (Figure 9). TEM showed that swelling podocytes in HFD mice had irregular shapes with flattened foot process, which were prevented by semaglutide. TEM revealed the disruption of the normal foot process ultrastructure in HFD mice, which was the wider foot process and even fused. Swelling endothelial cells separated from the basement membrane. The cell body of NFD podocytes contained abundant rough endoplasmic reticulum (RER) and many mitochondria. However, there were a loss of cristae membranes and reduced matrix density with mitochondria in HFD group. RER was less in number, and slightly expanded in local areas in HFD group. The basement membrane was locally slightly thickened in HFD group. In contrast, podocytes from HFD mice treated with semaglutide showed a normal density of cellular organelles and mitochondria with normal matrix density and cristae membranes (Figure 10).

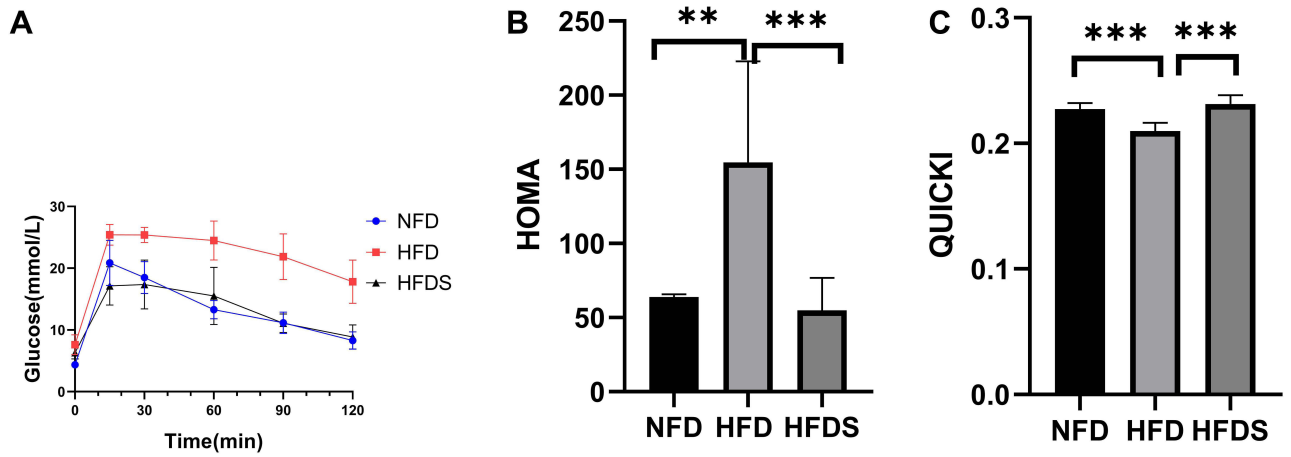

Figure 7 Effect of semaglutide on glucose homeostasis and insulin resistance. Means data from each group (n=8/group) are displayed **P<0.01, ***P<0.001, compared with NFD or HFD group. (**A**) Blood glucose levels at different times in each group. (**B**) HOMA index in each group. (**C**) QUICKI in each group.

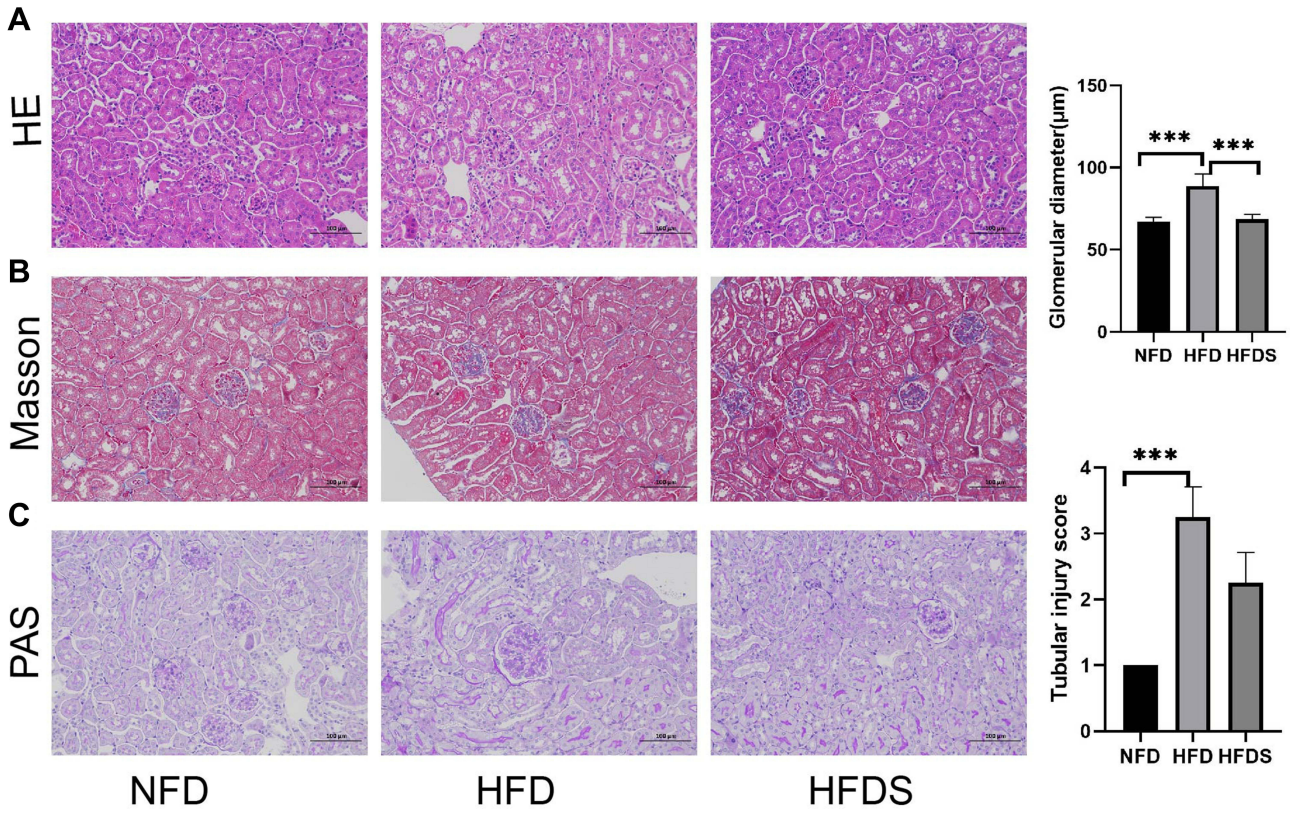

Figure 8 Semaglutide alleviated HFD-induced glomerular and tubular injury. (**A**) HE staining (×200 magnification). (**B**) Masson staining (×200 magnification). (**C**) PAS staining (×200 magnification). ***P<0.001, compared with NFD or HFD group.

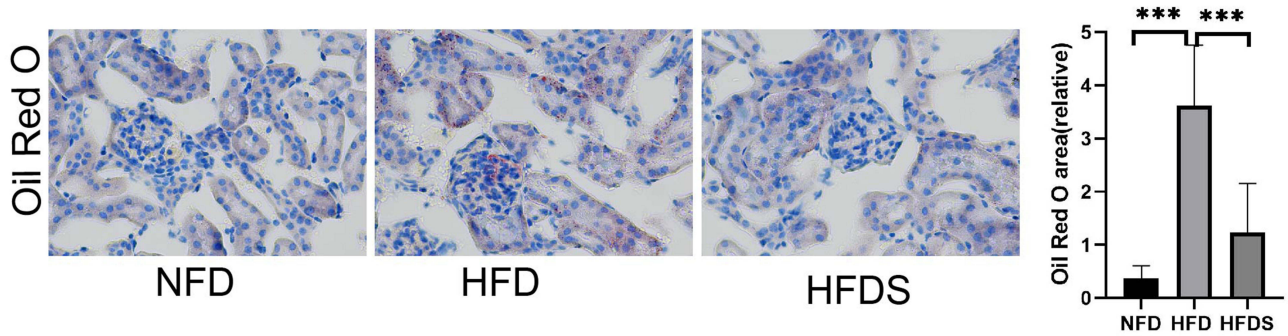

Figure 9 Semaglutide attenuated oil red O-stained lipid droplets observed in HFD mice. Oil red O staining (×400 magnification). ***P<0.001, compared with NFD or HFD group.

Effect of Semaglutide on Renal Metabolomics

Multivariate Analysis and Validation of LC-MS

For repeatable and high-quality data, we applied PCA and OPLS-DA as a pragmatic solution. PCA was an unsupervised method, which could visualize metabolic differences between groups. The PCA score plots (Figure 11) illustrated that the system was stable during sample analysis. The metabolic profiles between groups were significantly different. Based on supervised pattern recognition, the OPLS-DA model was designed to maximize separation and recognize potential biomarkers. As Figure 12 shows, the OPLS-DA score plot suggested that all groups were distinguished clearly. The model's goodness of fit R2Y and the goodness of prediction Q2 were R2Y=0.855, Q2=0.524, indicating a well-fitting OPLS-DA model. All these results showed that the LC-MS system was robust with good stability and reproducibility. Each point in the S-plot represented a metabolite. The farther from origin the point was, the greater influence it brought, as well as the higher VIP value. Metabolites with VIP value of more than 1 and P-value less than 0.05 in *t*-test were considered as potential biomarkers.

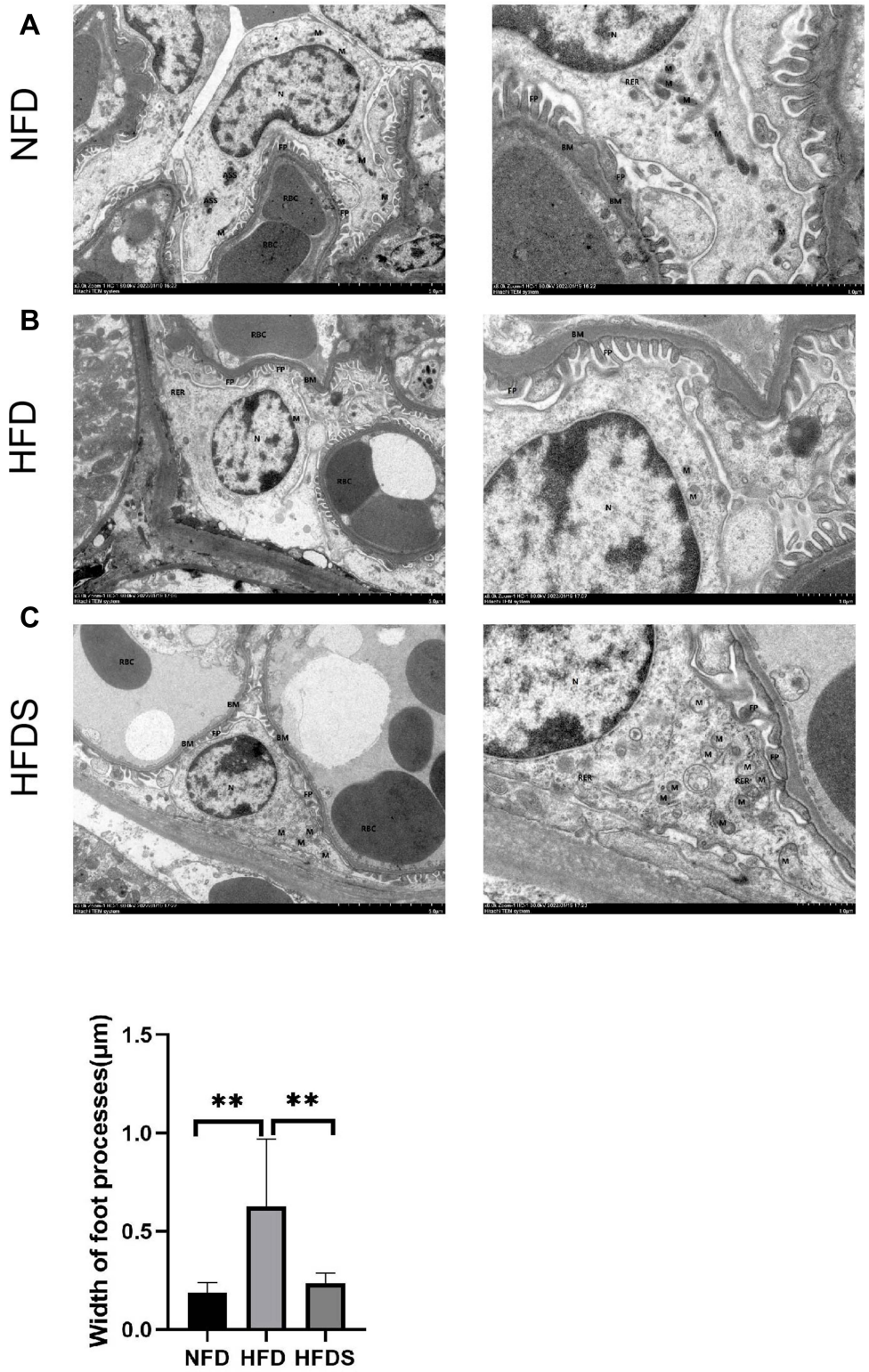

Figure 10 Semaglutide attenuated HFD-induced podocyte and mitochondria injury. **P<0.01, compared with NFD or HFD group. (**A**) Representative images of podocyte and mitochondria by electron microscopy in NFD group. (**B**) Representative images of podocyte and mitochondria by electron microscopy in HFD group. (**C**) Representative images of podocyte and mitochondria by electron microscopy in HFDS group.

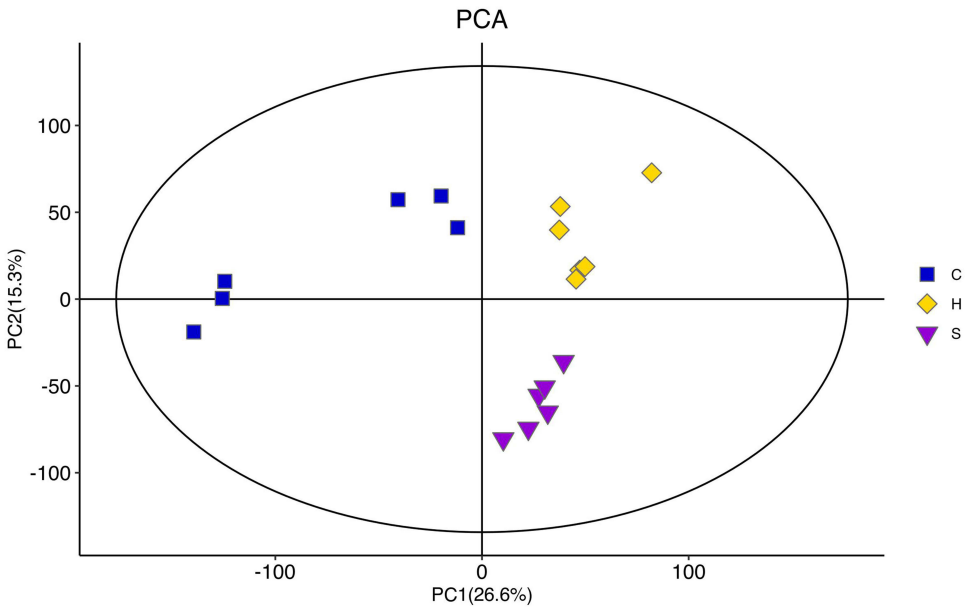

Figure 11 PCA of untargeted metabolite profiles. (C) NFD group, (H) HFD group, (S) HFDS group.

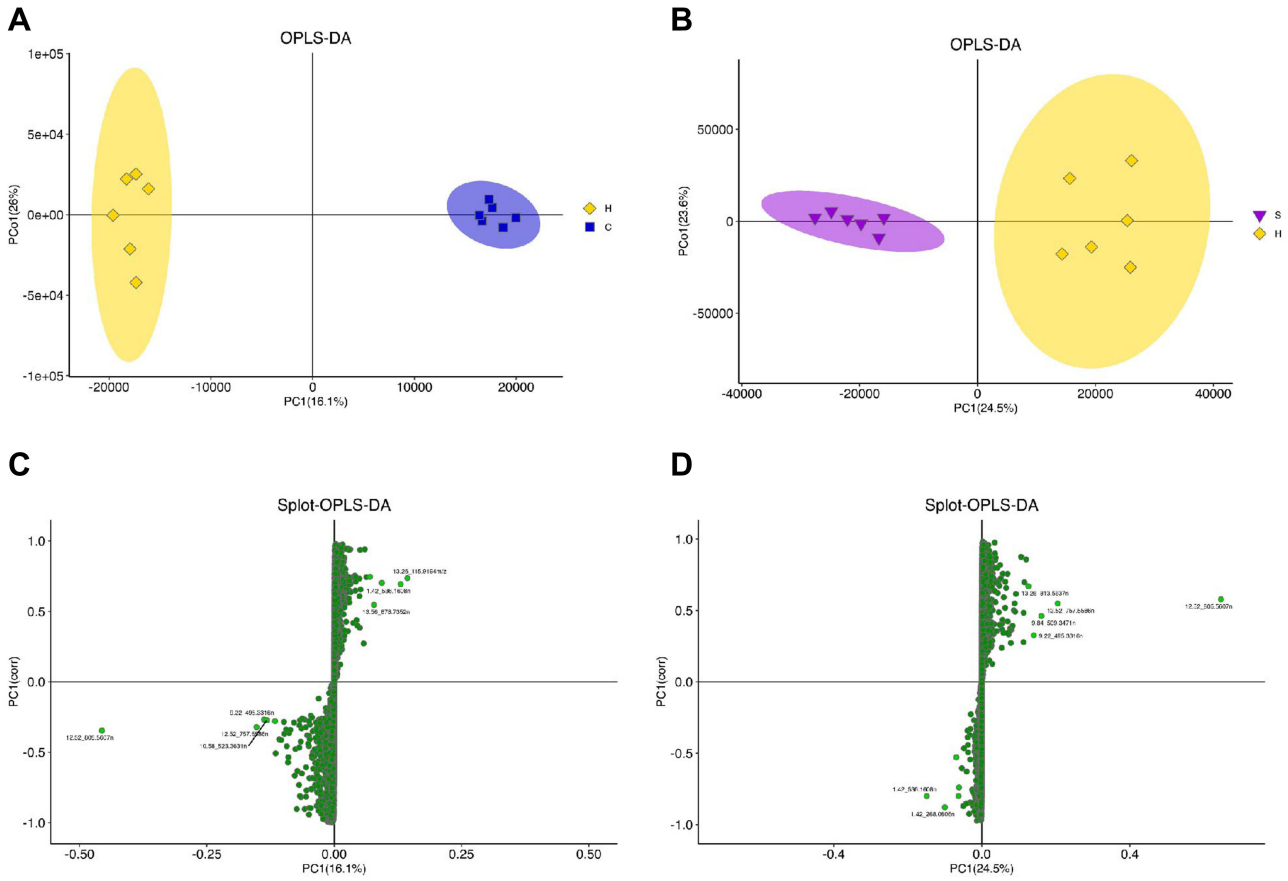

Figure 12 OPLS-DA score plots and S-plots of renal metabolic profiling between NFD group vs HFD group. (**A** and **C**)/ HFD group vs (**B** and **D**) HFDS group.

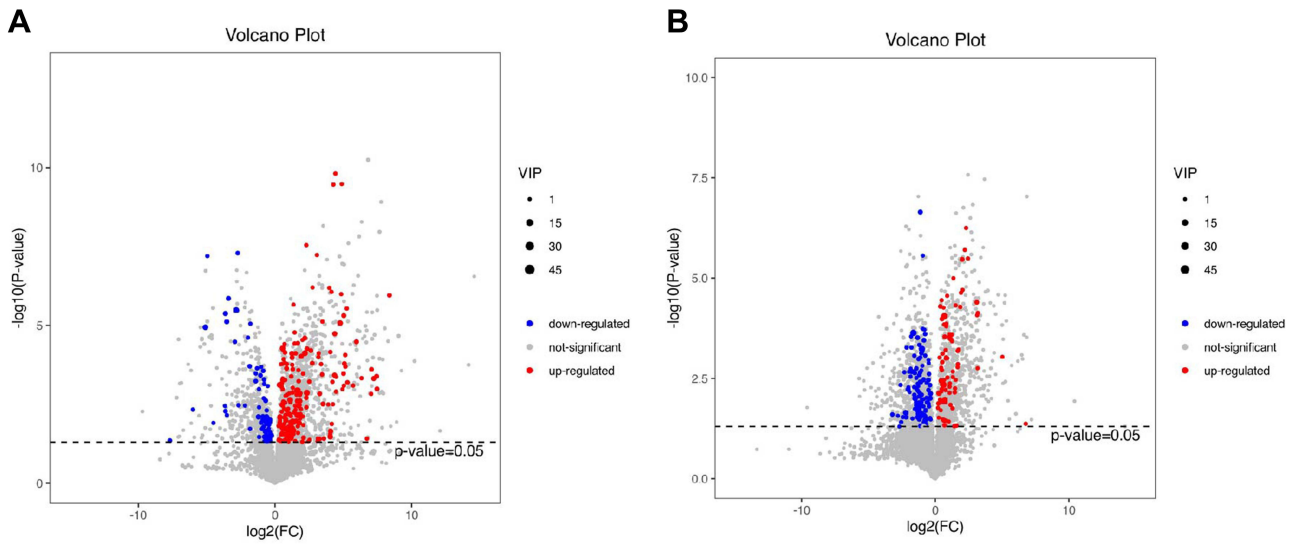

Figure 13 Volcano plot of renal metabolic profiling between NFD group vs HFD group (**A**)/HFD group vs HFDS group (**B**). The red dot represents significantly up-regulated metabolite, the blue dot represents significantly down-regulated metabolite, and the gray dot represents insignificant metabolite.

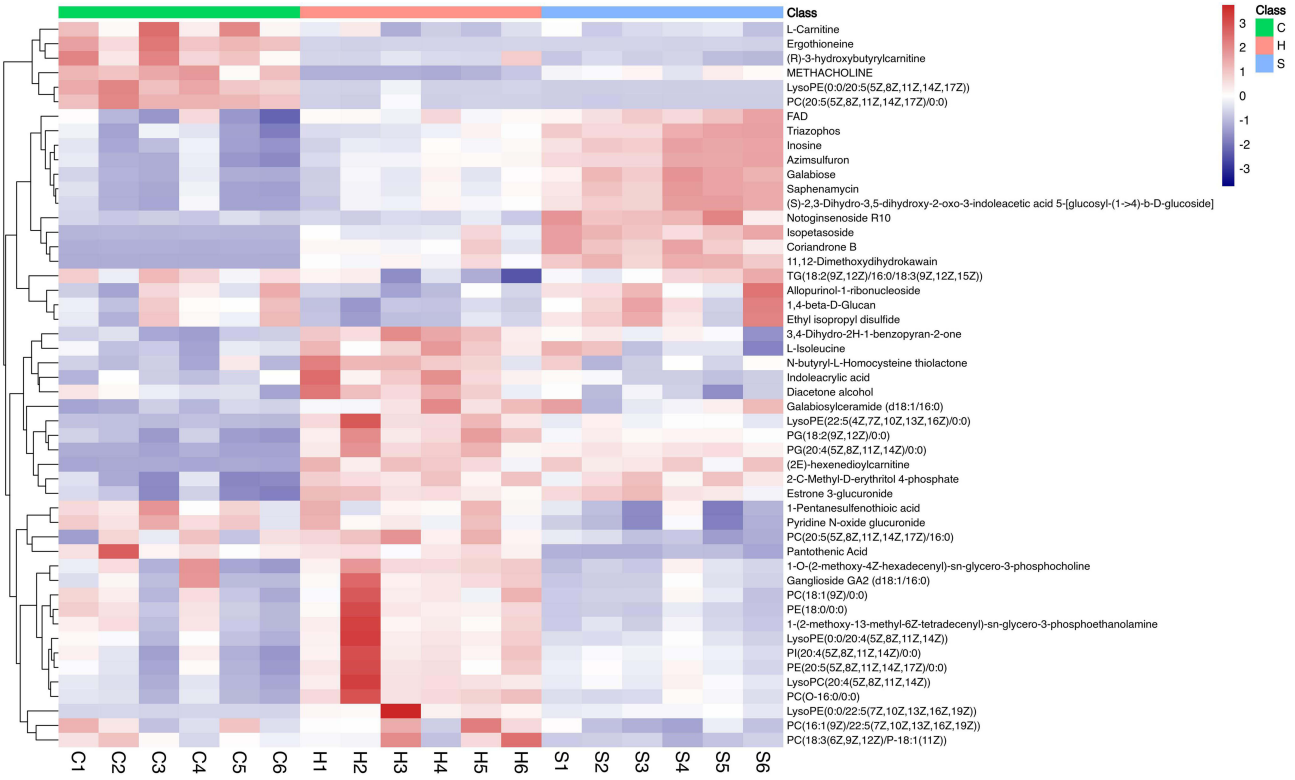

Figure 14 Hierarchical clustering heat map. (C) NFD group, (H) HFD group, (S) HFDS group. The abscissa represents the sample name and the ordinate represents the differential metabolites. The color from blue to red indicates the expression abundance of metabolites from low to high.

Identification and Quantitative Analysis of Renal Metabolites

Metabolic alterations in kidney tissues shed light on mechanisms contributing to ORG. A total of 377 statistically significant endogenous metabolites were identified in kidneys ($P<0.05$). The up-regulated or down-regulated metabolite profile between groups can be detected from the volcano map in Figure 13. Hierarchical clustering heat map (Figure 14) showed the relationship between samples and the expression differences of metabolites among different samples. We screened out 97

Table 2 Identification and the Change Trend of Metabolites

Identification	RT (Min)	Measured Mass (Da)	Mass Error (ppm)	Formular	Average (ND)	Average (HFD)	Average (HFDS)	VIP	*P*-value
1,4-beta-D-Glucan	1.42	559.15	3.54	C18H32O18	65,369,617.90	48,857,333.00	74,318,348.30	13.42	0.01
11,12-Epoxyeicosatrienoic acid	9.80	319.23	−0.11	C20H32O3	167,481.00	407,495.01	177,941.70	1.53	<0.001
Adenosine	1.27	268.10	−1.59	C10H13N5O4	1,370,252.79	919,528.25	1,359,705.27	2.13	0.02
Adenosine 3'-monophosphate	1.16	348.07	−2.05	C10H14N5O7P	386875.91	286,103.57	474,093.50	1.18	0.01
D-4'-Phosphopantothenate	1.48	322.07	−1.469	C9H18NO8P	927704.77	1,175,796.35	697,507.92	2.28	<0.001
Asymmetric dimethylarginine	0.77	203.15	−0.83	C8H18N4O2	172,720.50	307,240.01	219,296.58	1.31	0.01
Guanosine	1.39	284.10	−1.65	C10H13N5O5	577,369.50	332,028.89	698,627.17	1.64	0.003
Indoleacrylic acid	3.31	188.07	−2.13	C11H9NO2	3,975,532.01	5,725,032.90	4,028,923.94	4.64	<0.001
LysoPA (18:0/0:0)	15.402	483.27	0.36	C21H43O7P	36683.27	180,354.24	66,568.92	1.32	0.001
LysoPE (0:0/20:4(5Z,8Z,11Z,14Z))	8.72	500.28	0.07	C25H44NO7P	4728368.51	10,215,160.04	5,082,197.73	7.49	0.01
LysoPE (22:5(4Z,7Z,10Z,13Z,16Z)/0:0)	9.18	526.29	−0.66	C27H46NO7P	38161.35	782,756.87	355,441.02	3.44	<0.001
METHACHOLINE	0.89	160.13	−1.67	C8H17NO2	2,965,631.40	413,444.05	1,673,104.43	6.67	<0.001
N-arachidonoyl taurine	12.52	410.24	−0.25	C22H37NO4S	33758.13	192,106.82	103,225.09	1.57	0.0002
Nicotinamide adenine dinucleotide (NAD)	0.83	664.12	−1.55	C21H27N7O14P2	316,727.49	203,503.40	359,178.02	1.02	0.006
N-linoleoyl taurine	12.52	386.24	0.15	C20H37NO4S	106447.28	242,114.36	91,045.56	1.11	0.01
PC (22:5(4Z,7Z,10Z,13Z,16Z)/0:0)	9.38	614.35	0.27	C30H52NO7P	2910.95	515,370.32	209,872.66	2.76	0.0003
PC (O-16:0/0:0)	9.56	526.35	−0.23	C24H52NO6P	1657370.18	5,093,635.99	2,371,165.05	6.55	0.0002
PC (P-18:0/0:0)	9.88	552.37	0.471104185	C26H54NO6P	266896.67	813,718.29	342,717.88	2.53	0.0002
PE (20:5(5Z,8Z,11Z,14Z,17Z)/0:0)	9.18	544.27	−0.06	C25H42NO7P	1835805.36	4,156,406.20	2,577,357.36	5.17	0.008
PE (22:5(4Z,7Z,10Z,13Z,16Z)/0:0)	9.34	526.29	−0.46	C27H46NO7P	4910.74	735,655.88	249,850.39	3.22	<0.001
PE (O-16:0/0:0)	9.49	438.30	0.65	C21H46NO6P	55297.67	269,334.45	74,592.56	1.49	0.0002
PE (P-16:0e/0:0)	9.54	436.28	−0.15	C21H44NO6P	767813.32	1,976,051.83	745,052.29	3.39	0.006
PG (18:2(9Z,12Z)/0:0)	11.08	507.27	−0.39	C24H45O9P	690864.16	3,136,507.17	2,111,440.98	6.73	<0.001
PI (20:4(5Z,8Z,11Z,14Z)/0:0)	10.31	619.29	0.10	C29H49O12P	4097682.19	8,237,500.87	5,212,178.98	6.68	0.01
PS (16:0/0:0)	10.01	496.27	0.12	C22H44NO9P	434844.70	1,062,458.63	367,896.70	2.65	0.001
Tetrahydro-2-methyl-3-furanol	0.77	120.10	0.72	C5H10O2	113,988.31	231,696.98	74,754.58	1.43	0.002
All-trans-heptaprenyl diphosphate	9.40	699.38	2.24	C35H60O7P2	4657.89	183,331.12	85,839.12	1.65	0.0002

https://doi.org/10.2147/DDDT.S383537

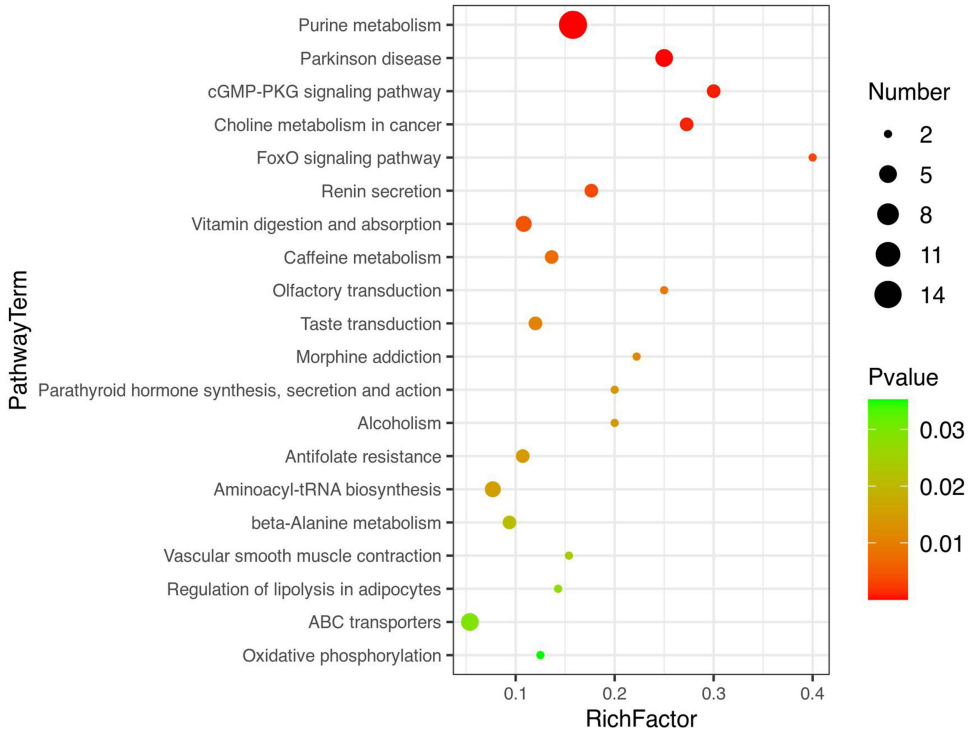

Figure 15 Bubble map of metabolic pathway.

metabolites that were simultaneously expressed in NFD group, HFD group and HFDS group. Then, we identified 27 metabolites that were up-regulated or down-regulated in HFD group and simultaneously expressed in the opposite direction in HFDS group according to VIP and P-value. The information of biomarkers is summarized in Table 2.

Disturbed Metabolic Pathways Involved

Integrated with multivariate analysis, metabolic pathways with $P<0.05$ were screened. Purine metabolism, ABC transporters, Renin secretion, FoxO signaling pathway, Aminoacyl−tRNA biosynthesis, and cGMP−PKG signaling pathway were the major metabolism pathways disturbed in obese mice. Metabolic pathways of Purine metabolism, Pantothenate and CoA biosynthesis, beta-Alanine metabolism, Vitamin digestion and absorption were involved after semaglutide intervention. By using the KEGG database, the following pathways were mainly involved, including lysophospholipids metabolism, purine metabolism, NAD metabolism, insulin resistance-related metabolism. The bubble diagram further explained the enrichment of metabolic pathways (Figure 15). The horizontal coordinate is the rich factor (rich factor = number of significantly differentiated metabolites/total metabolites in this pathway). The color from green to red indicated that P-value decreased successively. The larger the point was, the more metabolites were enriched into this pathway.

Correlation Analysis Between Clinicopathological Parameters and Metabolites

Spearman or Pearson's correlations between biochemical pathological parameters and identified metabolites were performed (Figure 16). Our analysis showed that UACR was related to 11,12-Epoxyeicosatrienoic acid, Adenosine, LysoPA (18:0/0:0), Asymmetric dimethylarginine Indoleacrylic acid, LysoPE (22:5 (4Z,7Z,10Z,13Z,16Z)/0:0), LysoPE (0:0/20:4 (5Z,8Z,11Z,14Z)), METHACHOLINE, Narachidonoyl taurine, Nicotinamide adenine dinucleotide (NAD), Nlinoleoyl taurine, PC (22:5 (4Z,7Z,10Z,13Z,16Z)/0:0), PC (O-16:0/0:0), PC (P-18:0/0:0), PE (P-16:0e/0:0), PE (O-16:0/0:0), PE (22:5 (4Z,7Z,10Z,13Z,16Z)/0:0), PE (20:5 (5Z,8Z,11Z,14Z,17Z)/0:0), PG (18:2 (9Z,12Z)/0:0), PI (20:4 (5Z,8Z,11Z,14Z)/0:0), PS (16:0/0:0), Tetrahydro-2-methyl-3-furanol, and All-trans-heptaprenyl diphosphate. As shown in Figure 16, metabolites in red or blue points represented correlations of positive or negative, respectively.

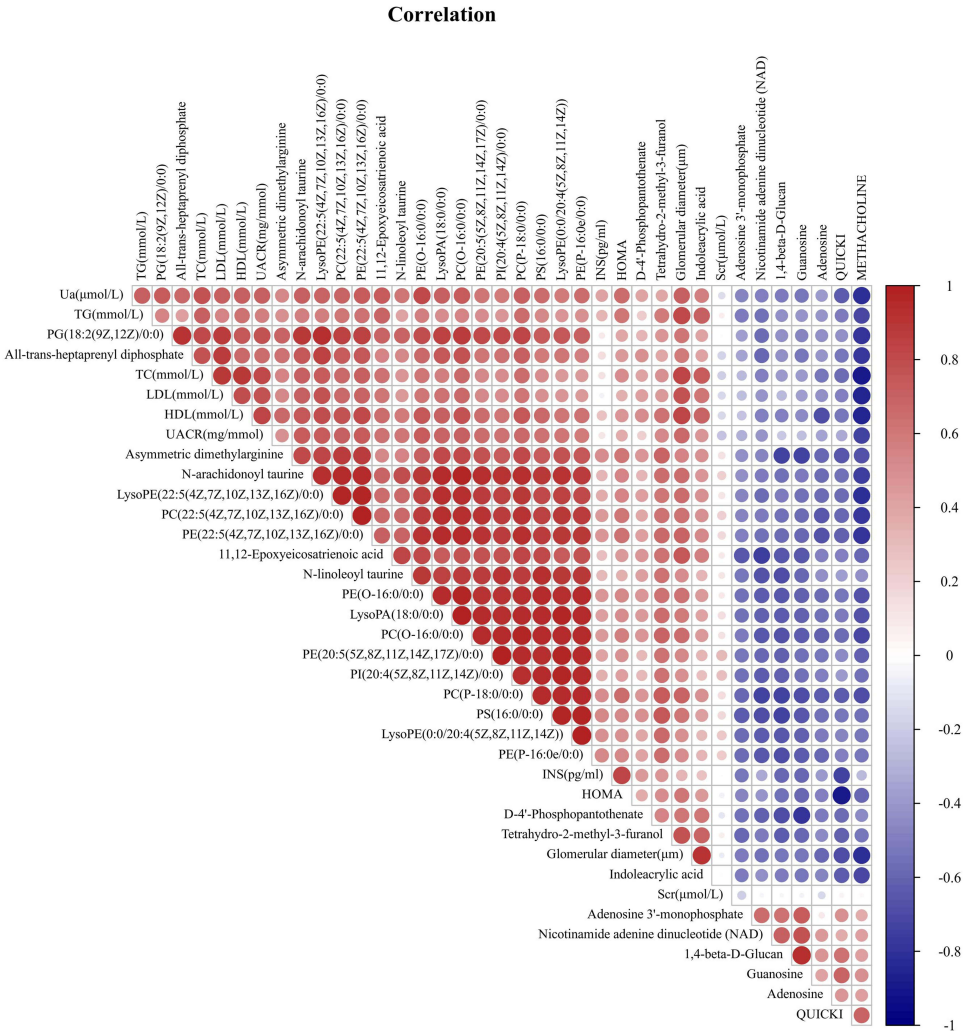

Figure 16 Heat map analysis of correlation between clinicopathological data and identified metabolites.

Adenosine participates in purine metabolism and NAD is involved in mitochondrial energy metabolism, which are all related to inflammatory response and oxidative stress correspondingly. For the rest metabolites, Adenosine 3'-monophosphate, Asymmetric dimethylarginine, Guanosine, Indoleacrylic acid, N-linoleoyl taurine are all related to the inflammatory response.[6,30–33] 11, 12-Epoxyeicosatrienoic acid, Guanosine, Adenosine, and Adenosine 3'-monophosphate are associated with oxidative stress.[34–39] For verification of downstream physiological effects, we further assayed inflammatory and oxidative stress parameters.

Effect of Semaglutide on Inflammation and Oxidative Stress

To explore whether semaglutide could alleviate the oxidative–antioxidative imbalance in obese mice, we measured SOD and MDA levels in serum. As expected, mice in HFD group exhibited reduced SOD activity ($P<0.001$) and elevated MDA levels ($P<0.001$), indicating excessive oxidative stress. However, semaglutide significantly enhanced SOD activity ($P=0.002$) and reduced renal MDA levels ($P=0.001$), indicating the recovery of oxidative–antioxidative imbalance. We further evaluated the expression of inflammation-related factors, including TNF-α, IL6, and IL-1β in serum. As a result, all the inflammation-related parameters were significantly increased in HFD group, proving the occurrence of inflammatory response. After administration of semaglutide, the expression levels of TNF-α, IL6, and IL-1β were all significantly decreased ($P<0.05$), which revealed that semaglutide could inhibit the occurrence of inflammatory response (Figure 17).

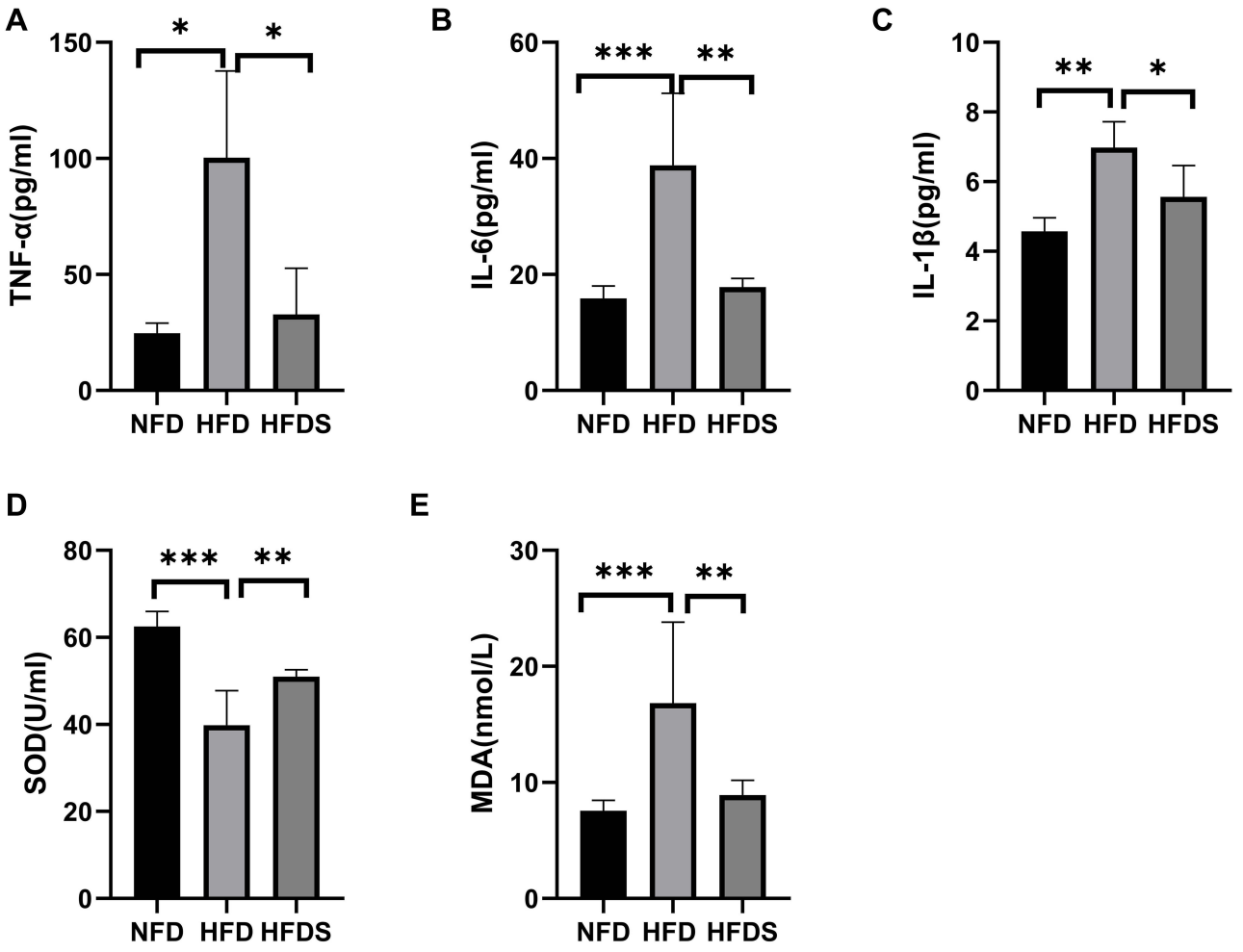

Figure 17 Semaglutide alleviated HFD–induced inflammation and oxidative Stress. Means data from each group (n=8/group) are displayed *P<0.05,**P<0.01,***P<0.001. (**A**) TNF-α in each group. (**B**) IL-6 in each group. (**C**) IL-1β in each group. (**D**) SOD in each group. (**E**) MDA in each group.

Discussion

Obesity has been one of the major health problems worldwide.[4,40–42] Increasing evidence shows that obesity poses an independently elevated risk of the CKD progression.[1,3,43,44] Glomerulopathy is the primary pathologic finding of obesity-related kidney disease. Lipid accumulation in the kidney causes oxidative stress and pro-inflammatory processes activation, which results in podocyte damage. Podocyte injury is the primary driving force in ORG progression.[5,8,13] HFD-induced obesity is pathophysiologically similar to obesity in humans. C57BL/6J mice are more sensitive to high-fat diets. Feeding a high-fat diet to C57BL/6J mice for 8–16 weeks is the most commonly used method for establishing the HFD model. Therefore, C57BL/6J mice are also called Diet-Induced Obesity mice. In addition, the model appears to display a pro-inflammatory state that is relevant to the human metabolic syndrome.[42,43,45] The model has been utilized widely in the evaluation of anti-obesity agents.

GLP-1, with a promising application prospect for the treatment of diabetes, is an incretin hormone secreted by secretory cells in the intestine.[5,46] The GLP-1 analog liraglutide has a half-life of approximately 12 hours in humans.[9–14] Semaglutide, with a sustained half-life of approximately one week, is marketed as a recent GLP-1 analog. Semaglutide is a modification of liraglutide by changing the amino acid at position 8, which can significantly reduce HbA1c and body weight. Semaglutide has been approved by the US Food and Drug Administration to treat obese people with comorbidities.[15,16,20,48–50] Previous studies revealed that semaglutide has a cardiovascular protective effect, which can

alleviate myocardial ischemia-reperfusion injury and myocardial infarction.[16] Although semaglutide is a longer-acting GLP-1 analog in humans, it has a shortened period of effectiveness in rodents.[17,20,49] Moreover, since the half-life of semaglutide in rodents is shorter than in humans, we selected dosing every day instead of once a week.

Metabolomics, the latest biology technology for understanding complex disease processes, focuses on the identification of biochemical signatures related to pathogenesis and diagnosis of disease. Changes at the genomic level may not be expressed, and thus will not affect the body system. The limitation of proteomics is that the relevant protein may not be active, and similarly will bring no effect. However, the production of small molecule metabolites is the result of a series of events. The advantages of metabolomics lie in the amplifying changes at the genetic level, making it easier to be identified. This is why we prefer to metabolomics.[8,21–24,51] There has been a lack of systematic metabolomics studies about the effect of semaglutide on ORG.

In our study, biochemical parameters suggested that obese mice had dyslipidemia and glucose metabolic disorders. Semaglutide significantly mitigated insulin resistance, lipid droplet deposition, glomerular and tubular injury. These results further confirmed the renal protective effect of semaglutide. We further verified the renoprotective mechanisms of semaglutide in obese mice using metabolomics. The following are the identified metabolic pathways.

Phospholipids (PLs) have different physiological functions depending on respective characteristics with a change in their head groups, such as Phosphatidyl choline (PC), Phosphatidyl ethanolamine (PE). PE is an important phospholipid in the membranes of animal cells. PLs are correlated with serum cholesterol level and renal function.[25,52] Lysophospholipids (LysoPLs) are produced by the action of phospholipase A, which are deacylated products of PLs with a single fatty acid chain. Several types of LysoPLs have been identified, including lysophosphatidic acid (LysoPA), lysophosphatidyl choline (Lyso PC), lysophosphatidyl ethanolamine (LysoPE), lysophosphatidyl glycerol (LysoPG), lysophosphatidyl inositol (LysoPI), and lysophosphatidyl serine (LysoPS). Their biological activities vary significantly. It is revealed that LysoPLs are associated with several diseases such as kidney injury, obesity, non-alcoholic fatty liver disease and cancer. LysoPC is the most abundant LysoPL in human plasma, and it is involved in vascular endothelial expansion, cellular immune response, and insulin secretion. Several studies have shown that LysoPEs are neurotrophic activators by activating mitogen-activated protein kinase (MAPK) signaling.[26,47,53] In our study, the levels of PLs and LysoPLs metabolites in the kidney of HFD group were significantly increased, indicating an imbalance of lipid metabolism in obese mice. Semaglutide improved lipid metabolism disorder.

Purinergic signaling has been shown to regulate physiological processes in kidney such as water and sodium homeostasis, renal blood flow autoregulation, tubular and glomerular functions. ATP and its ultimate degradation product adenosine are involved in purine metabolism signaling. Adenosine is an important paracrine inhibitor of inflammation.[6,37,54] Alterations in extracellular adenosine signaling can modulate immune responses, inflammatory processes and immunosuppression.[6,55] Adenosine activates four specific membrane adenosine receptors, which are named adenosine receptor A1 (A1AR), adenosine receptor A2A (A2AAR), adenosine receptor A2B (A2BAR), and adenosine receptor A3 (A3AR). These ARs belong to the family of G protein-coupled receptors. By inhibiting macrophage activation, adenosine can play an anti-inflammatory role. A2BAR regulate immunomodulatory and anti-inflammatory actions through inhibiting formation of IL-6 and transforming growth factor-beta 1 (TFG-β1). In addition to the regulation of inflammation, adenosine receptors have been linked to the mediation of glucose clearance. Adenosine analogue has also been reported to improve hyperglycemia status and reduce urinary protein excretion.[6,34,37,54,55] However, changes in adenosine levels of obesity-related nephropathy have not been reported. Our results showed that adenosine levels were decreased in obese mice, which were ameliorated after semaglutide administration.

NAD exists in two forms, including an oxidized (NAD^+) and a reduced (NADH) form. NAD^+ is involved in electron transport in mitochondria, which is required for oxidative phosphorylation and mitochondrial respiration.[36,56] Reduced NAD^+ levels are linked to aging, cancer, and neurodegenerative, metabolic syndrome and diabetes. Recent studies have also indicated that NAD^+ is essential in maintaining kidney health. NAD^+ metabolism is considered a therapeutic target for kidney disease.[35,36,56,57] Recently, Faivre et al found that impaired NAD^+ biosynthesis exacerbated acute kidney injury.[36] Our results showed that metabolites related to mitochondrial function changed, such as NAD and taurine, which

were well-known antioxidant substrates. Moreover, amelioration of mitochondrial function could be observed by TEM after semaglutide administration.

Our results revealed that decreased glucose tolerance and insulin resistance existed in obese mice. In our study, four identified metabolites were involved in insulin resistance: cholic acid, 5-l-glutamyl-taurine, glucosamine, and suberic acid.[29] As the VIP of 5-l-glutamyl-taurine, glucosamine, and suberic acid were less than 1, we did not further analyze the three metabolites in depth. Although the P-value of cholic acid was less than 0.05, there presented a trend of difference between groups. Research showed that insulin resistance was associated with decreased cholic acid, deoxycholic acid, and their conjugated forms.[29,58] It is reported that supplementation of high-fat obesogenic diets with cholic acid or chenodeoxycholic acid inhibits obesity development in mice.[55] Our results confirmed this point exactly.

UACR is the identification of kidney damage and dysfunction. The association between UACR and identified metabolites can be used to screen for specific biomarkers.[22,59] The highly negative correlations of adenosine and NAD levels with UACR indicated that nucleotide and energy metabolisms were closely related to the pathogenesis of ORG. These metabolites also could serve as potential biomarkers for drug targets of ORG. According to the screened metabolites, we further verified the indicators of inflammation and oxidative stress.

IL-1β and IL-6 are important mediators of inflammatory diseases, while TNF-α can further induce the production of inflammatory factors. Moreover, TNF-α level is associated with the degree of obesity and insulin resistance. In this experiment, semaglutide significantly reduced the expression of proinflammatory cytokines (IL-6, IL-1β and TNF-α).[3,16,21,32,60] Previous studies showed that oxidative stress response will result in accumulation of reactive oxygen and lipids deposit in tissue. Furthermore, lipid peroxidation can lead to final production of MDA, which subsequently cause severe cytotoxicity. SOD is known as a key antioxidant enzyme with functions of clearing free radicals and reducing oxidative stress.[16,21] This study adopted oil-red O staining to observe the effect of semaglutide on the lipid accumulation of renal tissue. As expected, semaglutide could significantly reduce the accumulation of lipid in kidney tissue and alleviate oxidation and antioxidant imbalance. Previous studies have also reported that semaglutide may improve cardiomyopathy and neurological diseases by inhibiting inflammation and oxidative stress. The result is consistent with our study.[15–17]

The present results highlight the renoprotective effects of semaglutide in obese mice based on metabolomics. However, there exist a couple of limitations in the research. Additional focused experiments are required to determine substrate sources for key metabolites and metabolic pathways involved. So our research team wants to make further research at different levels. Until now, there have been no related reports about the renoprotective mechanism of semaglutide in vitro experiments. We are going to utilize the intervention targets identified based on renal metabolomics for further mechanistic research at the cellular level.

Metabolomics provides new insights into the mechanism about renoprotection of semaglutide in ORG. In conclusion, the targeted molecular pathways, including Phospholipids and Lysophospholipids metabolism, Purine metabolism, NAD metabolism, and Insulin resistance-related metabolism, may be involved in the renal protective effects of semaglutide. This study suggested that semaglutide was a promising therapy for obesity-associated CKD.

Abbreviations

CKD, chronic kidney disease; ORG, obesity-related glomerulopathy; GLP-1, glucagon-like peptide-1; HFD, high-fat diet; Scr, serum creatinine; Ua, uric acid; TG, triglyceride; TC, total cholesterol; HDL, high-density lipoprotein; LDL, low-density lipoprotein; SOD, superoxide dismutase; MDA, malondialdehyde; IL-1β, interleukin-1β; IL-6, interleukin-6; TNF-α, tumor necrosis factor-α; NFD, normal-fat diet; UACR, urinary albumin/creatinine ratio; HOMA, homeostasis model assessment; QUICKI, Quantitative Insulin Sensitivity index; Ccr, creatinine clearance; HE, hematoxylin and eosin; PAS, periodic acid-Schiff; TEM, transmission electron microscopy; PCA, Principle Component Analysis; OPLS-DA, Orthogonal Partial Least-Squares-Discriminant Analysis; RER, rough endoplasmic reticulum; PLs, phospholipids; LysoPLs, lysophospholipids; NAD, nicotinamide adenine dinucleotide.

Data Sharing Statement

The metabolomics data are available from DOI: https://doi.org/10.5281/zenodo.6624467, URL: https://zenodo.org/record/6624467#.YqndFsiARB4.

Acknowledgments

The authors would like to thanks the Laboratory Animal Center in Hebei General Hospital for technical support.

Author Contributions

Shuchun Chen and Xing Chen planned experiments. Xing Chen wrote the manuscript. All authors made a significant contribution to the work reported, whether that is in the conception, study design, execution, acquisition of data, analysis and interpretation, or in all these areas; took part in drafting, revising or critically reviewing the article; gave final approval of the version to be published; have agreed on the journal to which the article has been submitted; and agree to be accountable for all aspects of the work.

Funding

The authors received no specific funding for this work.

Disclosure

The authors report no conflicts of interest in this work.

References

1. Gadde KM, Martin CK, Berthoud HR, et al. Obesity: pathophysiology and management. *J Am Coll Cardiol*. 2018;71(1):69–84.
2. Andres-Hernando A, Lanaspa MA, Kuwabara M, et al. Obesity causes renal mitochondrial dysfunction and energy imbalance and accelerates chronic kidney disease in mice. *Am J Physiol Renal Physiol*. 2019;317(4):F941–F948. doi:10.1152/ajprenal.00203.2019
3. Declèves AE, Sharma K. Obesity and kidney disease: differential effects of obesity on adipose tissue and kidney inflammation and fibrosis. *Curr Opin Nephrol Hypertens*. 2015;24(1):28–36. doi:10.1097/MNH.0000000000000087
4. McPherson KC, Shields CA, Poudel B, et al. Impact of obesity as an independent risk factor for the development of renal injury: implications from rat models of obesity. *Am J Physiol Renal Physiol*. 2019;316(2):F316–F327. doi:10.1152/ajprenal.00162.2018
5. Guo H, Wang B, Li H, et al. Glucagon-like peptide-1 analog prevents obesity-related glomerulopathy by inhibiting excessive autophagy in podocytes. *American Journal of Physiology. Renal Physiology*. 2018;314(2):F181–F189. doi:10.1152/ajprenal.00302.2017
6. Zhu JJ, Chen YP, Yang M, et al. Aldosterone is involved in the pathogenesis of obesity-related glomerulopathy through activation of Wnt/β-catenin signaling in podocytes. *Mol Med Rep*. 2018;17(3):4589–4598. doi:10.3892/mmr.2018.8386
7. Hsu WC, Lin CS, Chen JF, et al. The effects of dipeptidyl peptidase 4 inhibitors on renal function in patients with type 2 diabetes mellitus. *J Clin Med*. 2022;11(9):2653. doi:10.3390/jcm11092653
8. Kuwahara S, Hosojima M, Kaneko R, et al. Megalin-mediated tubuloglomerular alterations in high-fat diet-induced kidney disease. *JASN*. 2016;27(7):1996–2008. doi:10.1681/ASN.2015020190
9. Zhou JY, Poudel A, Welchko R, et al. Liraglutide improves insulin sensitivity in high fat diet induced diabetic mice through multiple pathways. *Eur J Pharmacol*. 2019;861:172594. doi:10.1016/j.ejphar.2019.172594
10. Le TD, Nguyen NPT, Nguyen ST, et al. The association between femoral artery intima-media thickness and serum glucagon-like peptide-1 levels among newly diagnosed patients with type 2 diabetes mellitus. *Diabetes Metab Syndr Obes*. 2020;13:3561–3570. doi:10.2147/DMSO.S264876
11. Sheikh A. Direct cardiovascular effects of glucagon like peptide-1. *Sheikh Diabetol Metab Syndr*. 2013;5:47. doi:10.1186/1758-5996-5-47
12. Le TD, Nguyen NPT, Tran HTT, et al. Diabetic peripheral neuropathy associated with cardiovascular risk factors and glucagon-like peptide-1 concentrations among newly diagnosed patients with type 2 diabetes mellitus. *Diabetes Metab Syndr Obes*. 2022;15:35–44. doi:10.2147/DMSO.S344532
13. Li K, Sun J, Huang N, et al. Liraglutide improves obesity-induced renal injury by alleviating uncoupling of the glomerular VEGF-NO axis in obese mice. *Clin Exp Pharmacol Physiol*. 2020;47(12):1978–1984. doi:10.1111/1440-1681.13391
14. Luo Y, Yang P, Li Z, et al. Liraglutide improves non-alcoholic fatty liver disease in diabetic mice by modulating inflammatory signaling pathways. *Drug Des Devel Ther*. 2019;13:4065–4074. doi:10.2147/DDDT.S224688
15. Zhang L, Zhang L, Li L, et al. Semaglutide is neuroprotective and reduces α-synuclein levels in the chronic MPTP mouse model of Parkinson's disease. *J Parkinson's Dis*. 2019;9(1):157–171. doi:10.3233/JPD-181503
16. Li Q, Tuo X, Li B, et al. Semaglutide attenuates excessive exercise-induced myocardial injury through inhibiting oxidative stress and inflammation in rats. *Life Sci*. 2020;250:117531. doi:10.1016/j.lfs.2020.117531
17. Basalay MV, Davidson SM, Yellon DM. Neuroprotection in rats following ischaemia-reperfusion injury by GLP-1 analogues-liraglutide and semaglutide. *Cardiovasc Drugs Ther*. 2019;33(6):661–667. doi:10.1007/s10557-019-06915-8
18. Pontes-da-Silva RM, de Souza Marinho T, de Macedo Cardoso LE, et al. Obese mice weight loss role on nonalcoholic fatty liver disease and endoplasmic reticulum stress treated by a GLP-1 receptor agonist. *Int J Obes*. 2022;46(1):21–29. doi:10.1038/s41366-021-00955-7
19. Rakipovski G, Rolin B, Nøhr J, et al. The GLP-1 analogs liraglutide and semaglutide reduce atherosclerosis in ApoE (-/-) and LDLr (-/-) mice by a mechanism that includes inflammatory pathways. *JACC*. 2018;3(6):844–857. doi:10.1016/j.jacbts.2018.09.004
20. Lau J, Bloch P, Schäffer L, et al. Discovery of the once-weekly glucagon-like peptide-1 (GLP-1) analogue semaglutide. *J Med Chem*. 2015;58(18):7370–7380. doi:10.1021/acs.jmedchem.5b00726
21. Liu J, Wang C, Liu F, et al. Metabonomics revealed xanthine oxidase-induced oxidative stress and inflammation in the pathogenesis of diabetic nephropathy. *Anal Bioanal Chem*. 2015;407(9):2569–2579. doi:10.1007/s00216-015-8481-0
22. Wei T, Zhao L, Jia J, et al. Metabonomic analysis of potential biomarkers and drug targets involved in diabetic nephropathy mice. *Sci Rep*. 2015;5:11998. doi:10.1038/srep11998

23. Mulder S, Hammarstedt A, Nagaraj SB, et al. A metabolomics-based molecular pathway analysis of how the sodium-glucose co-transporter-2 inhibitor dapagliflozin may slow kidney function decline in patients with diabetes. *Diabetes Obes Metab*. 2020;22(7):1157–1166. doi:10.1111/dom.14018
24. Chen H, Cao G, Chen DQ, et al. Metabolomics insights into activated redox signaling and lipid metabolism dysfunction in chronic kidney disease progression. *Redox Biol*. 2016;10:168–178. doi:10.1016/j.redox.2016.09.014
25. Airaksinen K, Jokkala J, Ahonen I, et al. High-fat diet, betaine, and polydextrose induce changes in adipose tissue inflammation and metabolism in C57BL/6J mice. *Mol Nutr Food Res*. 2018;62(23):e1800455. doi:10.1002/mnfr.201800455
26. Cheng L, Zhang S, Shang F, et al. Emodin improves glucose and lipid metabolism disorders in obese mice via activating brown adipose tissue and inducing browning of white adipose tissue. *Front Endocrinol*. 2021;12:618037. doi:10.3389/fendo.2021.618037
27. Sun X, Han F, Lu Q, et al. empagliflozin ameliorates obesity-related cardiac dysfunction by regulating sestrin2-mediated AMPK-mTOR signaling and redox homeostasis in high-fat diet-induced obese mice. *Diabetes*. 2020;69(6):1292–1305. doi:10.2337/db19-0991
28. Wang D, Liu J, He S, et al. Assessment of early renal damage in diabetic rhesus monkeys. *Endocrine*. 2014;47(3):783–792. doi:10.1007/s12020-014-0211-4
29. Men L, Pi Z, Zhou Y, et al. Urine metabolomics of high-fat diet induced obesity using UHPLC-Q-TOF-MS. *J Pharm Biomed Anal*. 2017;132:258–266. doi:10.1016/j.jpba.2016.10.012
30. Ding S, Jiang H, Fang J, et al. Regulatory effect of resveratrol on inflammation induced by lipopolysaccharides via reprogramming intestinal microbes and ameliorating serum metabolism profiles. *Front Immunol*. 2021;12:777159. doi:10.3389/fimmu.2021.777159
31. Wlodarska M, Luo C, Kolde R, et al. Indoleacrylic acid produced by commensal peptostreptococcus species suppresses inflammation. *Cell Host Microbe*. 2017;22(1):25–37. doi:10.1016/j.chom.2017.06.007
32. Luo Y, Chen H, Huang R, et al. Guanosine and uridine alleviate airway inflammation via inhibition of the MAPK and NF-κB signals in OVA-induced asthmatic mice. *Pulm Pharmacol Ther*. 2021;69:102049. doi:10.1016/j.pupt.2021.102049
33. Huang S, Xu Y, Peng WF, et al. Asymmetric dimethylarginine targets MAPK pathway to regulate insulin resistance in liver by activating inflammation factors. *J Cell Biochem*. 2018;2018:1.
34. Dwyer KM, Kishore BK, Robson SC. Conversion of extracellular ATP into adenosine: a master switch in renal health and disease. *Nat Rev Nephrol*. 2020;16(9):509–524.
35. Amjad S, Nisar S, Bhat AA, et al. Role of NAD (+) in regulating cellular and metabolic signaling pathways. *Mol Metab*. 2021;49:101195. doi:10.1016/j.molmet.2021.101195
36. Faivre A, Katsyuba E, Verissimo T, et al. Differential role of nicotinamide adenine dinucleotide deficiency in acute and chronic kidney disease. *Nephrol Dial Transplant*. 2021;36(1):60–68. doi:10.1093/ndt/gfaa124
37. Pandey S, Aggarwal D, Gupta K, et al. "Adenosine an old player with new possibilities in kidney diseases": preclinical evidences and clinical perspectives. *Life Sci*. 2021;265:118834. doi:10.1016/j.lfs.2020.118834
38. Liu T, Li T, Chen X, et al. EETs/sEHi alleviates nociception by blocking the crosslink between endoplasmic reticulum stress and neuroinflammation in a central poststroke pain model. *J Neuroinflammation*. 2021;18(1):211. doi:10.1186/s12974-021-02255-3
39. Samala N, Tersey SA, Chalasani N, et al. Molecular mechanisms of nonalcoholic fatty liver disease: potential role for 12-lipoxygenase. *J Diabetes Complications*. 2017;31(11):1630–1637. doi:10.1016/j.jdiacomp.2017.07.014
40. Câmara NO, Iseki K, Kramer H, et al. Kidney disease and obesity: epidemiology, mechanisms and treatment. *Nature Reviews. Nephrology*. 2017;13(3):181–190. doi:10.1038/nrneph.2016.191
41. Bovet P, Chiolero A, Gedeon J. Health effects of overweight and obesity in 195 countries. *N Engl J Med*. 2017;377(15):1495–1496.
42. Wong SK, Chin KY, Suhaimi FH, et al. Animal models of metabolic syndrome: a review. *Nutr Metab*. 2016;13:65. doi:10.1186/s12986-016-0123-9
43. Mouton AJ, Li X, Hall ME, et al. Obesity, hypertension, and cardiac dysfunction: novel roles of immunometabolism in macrophage activation and inflammation. *Circ Res*. 2020;126(6):789–806. doi:10.1161/CIRCRESAHA.119.312321
44. Carbone A, Al Salhi Y, Tasca A, et al. Obesity and kidney stone disease: a systematic review. *Minerva urologica e nefrologica*. 2018;70(4):393–400. doi:10.23736/S0393-2249.18.03113-2
45. Oh H, Jeong KH, Han HY, et al. A potent and selective 11β-hydroxysteroid dehydrogenase type 1 inhibitor, SKI2852, ameliorates metabolic syndrome in diabetic mice models. *Eur J Pharmacol*. 2015;768:139–148. doi:10.1016/j.ejphar.2015.10.042
46. Kim GW, Lin JE, Snook AE, et al. Calorie-induced ER stress suppresses uroguanylin satiety signaling in diet-induced obesity. *Nutr Diabetes*. 2016;6(5):e211. doi:10.1038/nutd.2016.18
47. Wang C, Li L, Liu S, et al. GLP-1 receptor agonist ameliorates obesity-induced chronic kidney injury via restoring renal metabolism homeostasis. *PLoS One*. 2018;13(3):e0193473. doi:10.1371/journal.pone.0193473
48. Newsome PN, Buchholtz K, Cusi K, et al. A placebo-controlled trial of subcutaneous semaglutide in nonalcoholic steatohepatitis. *N Engl J Med*. 2021;384(12):1113–1124. doi:10.1056/NEJMoa2028395
49. Nadolsky KZ, Agarwal M. Once-weekly semaglutide in adults with overweight or obesity. *N Engl J Med*. 2021;385(1):e4.
50. Zhang L, Zhang L, Li L, et al. Neuroprotective effects of the novel GLP-1 long acting analogue semaglutide in the MPTP Parkinson's disease mouse model. *Neuropeptides*. 2018;71:70–80. doi:10.1016/j.npep.2018.07.003
51. Suh DH, Lee HW, Jung ES, et al. In vivo metabolomic interpretation of the anti-obesity effects of hyacinth bean (Dolichos lablab L.) administration in high-fat diet mice. *Mol Nutr Food Res*. 2017;61(8). doi:10.1002/mnfr.201600895
52. Shon JC, Kim WC, Ryu R, et al. Plasma lipidomics reveals insights into anti-obesity effect of chrysanthemum morifolium Ramat leaves and its constituent luteolin in high-fat diet-induced dyslipidemic mice. *Nutrients*. 2020;12(10):2973. doi:10.3390/nu12102973
53. Yamamoto Y, Sakurai T, Chen Z, et al. Analysis of serum lysophosphatidylethanolamine levels in patients with non-alcoholic fatty liver disease by liquid chromatography-tandem mass spectrometry. *Anal Bioanal Chem*. 2021;413(1):245–254. doi:10.1007/s00216-020-02996-9
54. Johnston-Cox H, Koupenova M, Yang D, et al. The A2b adenosine receptor modulates glucose homeostasis and obesity. *PLoS One*. 2012;7(7):e40584. doi:10.1371/journal.pone.0040584
55. Pak ES, Jeong LS, Hou X, et al. Dual actions of A (2A) and A (3) adenosine receptor ligand prevents obstruction-induced kidney fibrosis in mice. *Int J Mol Sci*. 2021;22(11):5667. doi:10.3390/ijms22115667
56. Covarrubias AJ, Perrone R, Grozio A, et al. NAD (+) metabolism and its roles in cellular processes during ageing. *Nat Rev Mol Cell Biol*. 2021;22(2):119–141. doi:10.1038/s41580-020-00313-x

57. Liu X, Luo D, Huang S, et al. Impaired nicotinamide adenine dinucleotide biosynthesis in the kidney of chronic kidney disease. *Front Physiol*. 2021;12:723690. doi:10.3389/fphys.2021.723690
58. Ippagunta SM, Kharitonenkov A, Adams AC, et al. Cholic acid supplementation of a high-fat obesogenic diet suppresses hepatic triacylglycerol accumulation in mice via a fibroblast growth factor 21-dependent mechanism. *J Nutr*. 2018;148(4):510–517. doi:10.1093/jn/nxy022
59. Li M, Wang X, Aa J, et al. GC/TOFMS analysis of metabolites in serum and urine reveals metabolic perturbation of TCA cycle in db/db mice involved in diabetic nephropathy. *Am J Physiol Renal Physiol*. 2013;304(11):F1317–1324. doi:10.1152/ajprenal.00536.2012
60. Akash MSH, Rehman K, Liaqat A. Tumor necrosis factor-alpha: role in development of insulin resistance and pathogenesis of type 2 diabetes mellitus. *J Cell Biochem*. 2018;119(1):105–110. doi:10.1002/jcb.26174